Structural Changes of the Cry1Ac Oligomeric Pre-Pore from *Bacillus thuringiensis* Induced by *N*-Acetylgalactosamine Facilitates Toxin Membrane Insertion†

Liliana Pardo-López, Isabel Gómez, Carolina Rausell, Jorge Sánchez, Mario Soberón, and Alejandra Bravo*

Instituto de Biotecnologia, Universidad Nacional Autónoma de México, Apdo. Postal 510-3, Cuernavaca 62250, Morelos, Mexico

Received February 10, 2006; Revised Manuscript Received April 28, 2006

ABSTRACT: The primary action of Cry toxins produced by *Bacillus thuringiensis* is to lyse midgut epithelial cells in their target insect by forming lytic pores. The toxin−receptor interaction is a complex process, involving multiple interactions with different receptor and carbohydrate molecules. It has been proposed that Cry1A toxins sequentially interact with a cadherin receptor, leading to the formation of a pre-pore oligomer structure, and that the oligomeric structure binds to glycosylphosphatidyl-inositol-anchored aminopeptidase-N (APN) receptor. The Cry1Ac toxin specifically recognizes the *N*-acetylgalactosamine (GalNAc) carbohydrate present in the APN receptor from *Manduca sexta* larvae. In this work, we show that the Cry1Ac pre-pore oligomer has a higher binding affinity with APN than the monomeric toxin. The effects of GalNAc binding on the toxin structure were studied in the monomeric Cry1Ac, in the soluble pre-pore oligomeric structure, and in its membrane inserted state by recording the fluorescence status of the tryptophan (W) residues. Our results indicate that the W residues of Cry1Ac have a different exposure to the solvent when compared with that of the closely related Cry1Ab toxin. GalNAc binding specifically affects the exposure of W545 in the pre-pore oligomer in contrast to the monomer where GalNAc binding did not affect the fluorescence of the toxin. These results indicate a subtle conformational change in the GalNAc binding pocket in the pre-pore oligomer that could explain the increased binding affinity of the Cry1Ac pre-pore to APN. Although our analysis did not reveal major structural changes in the pore-forming domain I upon GalNAc binding, it showed that sugar interaction enhanced membrane insertion of soluble pre-pore oligomeric structure. Therefore, the data presented here permits to propose a model in which the interaction of Cry1Ac pre-pore oligomer with APN receptor facilitates membrane insertion and pore formation.

The major determinants of the *Bacillus thuringiensis* (Bt) insecticidal properties are the δ-endotoxins, also known as Cry and Cyt proteins (*1*). It is widely accepted that the primary action of Cry toxins is to lyse midgut epithelial cells in their target insects by forming lytic pores in the apical microvilli membrane (*1*−*3*). Upon crystal ingestion by the susceptible larvae, the solubilized inactive protoxins are cleaved by midgut proteases yielding 60−70 kDa protease resistant proteins (*4*). The activated toxin binds to specific receptors on the brush border membrane of the midgut columnar cells (*1*, *3*). It was proposed that the toxin−receptor interaction triggers toxin oligomerization resulting in the formation of a soluble pre-pore (*5*). The pre-pore inserts into the membrane, forming lytic pores (*6*). Cell lysis and the disruption of the midgut epithelium provide a rich medium suitable for spore germination leading to severe septicemia and insect death (*1*, *2*).

The crystal structures of several Cry toxins have been solved (*7*−*10*). The seven α-helices that form *N*-terminal domain I, have been implicated in the pore formation. Domain II consists of three antiparallel β-sheets with exposed loop regions, whereas domain III is a β-sandwich. Domains II and III are important in receptor recognition (*7*−*10*).

The toxin−receptor interaction is a complex process, involving multiple interactions with different receptor epitopes and carbohydrate molecules. In the case of the lepidopteran insect *Manduca sexta*, at least two Cry1A-binding proteins, a cadherin-like protein (Bt-R_1[1]) and a glycosylphosphatidyl-inositol (GPI) anchored aminopeptidase-N (APN), have been described as receptors of Cry1A toxins (*11*, *12*). Previously, we provided evidence that in *M. sexta* Cry1Ab toxin binding to Bt-R_1 and APN receptors depends on the toxin's oligomeric structure (*6*). The interaction of monomeric Cry1Ab toxin with Bt-R_1 is a critical step because it facilitates the formation of the pre-pore oligomer, which is the membrane insertion intermediate of the toxin (*5*). However, it has been suggested that APN could be involved in the localization of the toxin in membrane microdomains because after their interaction, both molecules (APN and the oligomeric Cry1Ab) were detected in insoluble membrane microdomains (*6*, *13*). Also, APN has been implicated in toxin insertion because

† This research was supported in part by DGAPA/UNAM IN207503-3, IN206503-3, USDA 2002-35302-12539, and NIH 1R01 AI066014-01.

* Corresponding author. Tel: 52-777-3291635. Fax: 52-777-3291624. E-mail: bravo@ibt.unam.mx.

[1] Abbreviations: GalNAc, *N*-acetylgalactosamine; GlcNAc, *N*-acetylglucosamine; Bt-R_1, cadherin-like protein; APN, aminopeptidase-N; W, tryptophan; GPI, glycosylphosphatidyl-inositol; SUV, small unilamellar vesicles; BBMV, brush border membrane vesicles.

10.1021/bi060297z CCC: $33.50
Published on Web 08/04/2006

cleavage of APN by phosphatidyl-inositol specific phospholipase C treatment substantially decreased the levels of the Cry1Ab oligomer in insoluble membranes (*6*) and drastically reduced the pore-formation activity of the toxin (*14*). In addition, APN incorporation into the lipid bilayer enhanced Cry1Aa pore-formation activity (*15*). Therefore, the interaction of the pre-pore oligomer of Cry1A toxins with APN could be important for the efficient membrane insertion of the pre-pore oligomer.

Interestingly, the Cry-receptors characterized so far are glycosilated proteins suggesting that carbohydrate interactions could also have a role in toxin−receptor recognition. Furthermore, the 3D structure of both binding domains (domain II and III) have a remarkable similarity to the topology of some carbohydrate-binding proteins (*16*). In the case of Cry1Ac toxin, the APN interaction is determined by *N*-acetylgalactosamine (GalNAc) carbohydrate binding, although this case is unique because the closely related Cry1Aa and Cry1Ab toxins do not interact with GalNAc (*17*, *18*). Besides APN, a recently characterized GPI-anchored alkaline phosphatase was proposed to be a functional receptor of Cry1Ac toxin in *Heliothis virescens*; this protein also contains the GalNAc moiety (*19*).

In the case of the lepidopteran insect *Lymantria dispar*, it was shown that two surface regions of the monomeric Cry1Ac toxin are involved in the interaction with APN, and a sequential binding model was proposed (*20*). In this model, APN recognition is determined by domain III binding through a GalNAc moiety on the APN receptor, followed by a contact of domain II loop region with APN. The first contact is fast and reversible, and mutations close to a domain III cavity affected this initial binding, whereas mutations in domain II affected the rate constants of the second interaction step, which is slower and tighter (*18*, *20*). Mutagenesis studies of Cry1Ac domain III identified residues ^{509}QNR^{511}, N^{506}, and Y^{513} as the sugar-binding epitope (*21*, *22*). In a review presented by Li et al. in 2001, the authors mentioned that the binding of GalNAc to monomeric Cry1Ac correlates with an increase of temperature factors in pore-forming domain I (*23*); however, there was no indication of a clear conformational change (*23*).

In this work, we aim to analyze the structural changes presented by the Cry1Ac toxin upon binding to the APN receptor and the role of this interaction in toxin membrane insertion. Because GalNAc is a binding determinant in the Cry1Ac−APN interaction, the structural changes induced by APN interaction were studied by analyzing the binding of Cry1Ac to GalNAc. The effects of GalNAc binding on the toxin structure were studied in the monomeric Cry1Ac as well as in the soluble pre-pore oligomeric structure and in its membrane inserted state by recording the fluorescence status of the W. Cry1Ac has ten W residues; eight of them are highly conserved among the members of the Cry three domain family (six located in domain I and two in domain II). The W219, which is located in α-helix 7, is only present in Cry1A toxins, whereas W545, located close to the domain III cavity that has been mapped at the GalNAc binding region, is only present in Cry1Ac toxin (*20*).

Our results indicate that the GalNAc induces a conformational change in domain III of the oligomeric structure of Cry1Ac. In addition, the interaction with the ligand sugar enhanced membrane insertion of soluble pre-pore oligomeric structure, supporting the model that the interaction of Cry1A pre-pore with GPI-anchored receptors facilitates membrane insertion and pore formation.

EXPERIMENTAL PROCEDURES

Site Directed Mutagenesis. The mutagenesis of the pHT3101 plasmid (*24*) harboring the *cry*1Ac gene (kindly supplied by Dr. A. Aronson, Purdue University) was performed using the QuikChange XL-kit (Stratagene, La Jolla, CA). W545 was substituted by alanine, and appropriate oligonucleotides were synthesized at the facilities of Instituto de Biotecnología, UNAM (upper primer 5′AGG ATT TAC TGG GGA CTT AG, lower primer 5′ATC ACT CCT GCA GTC CCA C). Mutant W545A was sequenced in both strands to confirm the presence of a single mutation.

Purification and Activation of Cry1Ac and the W545A Toxin. Crystal inclusions of Cry1Ac and mutant W545A were produced in the acrystalliferous Bt strain 407cry$^-$ transformed with pHT3101 or pHT3101-W545A plasmids, respectively. The transformed strains were grown for 3 days at 30 °C in nutrient broth sporulation medium supplemented with 10 μg/mL of erythromycin. After complete sporulation, the crystals were purified by sucrose gradients as reported (*25*) and solubilized in an extraction buffer (50 mM Na_2CO_3 at pH 10.5, 0.02% β-mercaptoethanol). The activation of protoxins was performed as described (*5*) by the incubation of Cry1Ac or W545A crystals with scFv73 antibody in a mass ratio of 1:1 and digestion with 1% (v/v) of *Manduca sexta* midgut juice for 1 h at 37 °C in the extraction buffer. PMSF was added to a final 1 mM concentration to stop proteolysis. The purification of monomeric and oligomeric structures of Cry1Ac or W545A toxins was achieved by size-exclusion chromatography with Superdex 200 HR 10/30 (Amersham Pharmacia Biotech, Uppsala, Sweden) FPLC size-exclusion as described (*26*).

Insect Bioassays. The toxicity of wild-type Cry1Ac toxin and mutant W545A was assayed in first instar *M. sexta* larvae. The larvae were fed with different doses from 0.25 to 100 ng/cm^2 of toxin on an artificial diet (Bio-Serv) in 24-well plaques (Cell Wells, Corning Glass Works, Corning, NY 14831). Bioassays were performed at 28 °C, 65 ± 5% relative humidity, and a light/dark photoperiod of 16:8 h. Mortality was recorded after 7 days and LC_{50} analyzed by Probit (Polo-PC LeOra Software).

Protein Concentration. Protein concentration was determined by Bradford assay using bovine serum albumin as the standard.

Preparation of Brush Border Membrane Vesicles (BBMV). BBMV from fifth instar *M. sexta* larvae were prepared and analyzed as previously reported (*27*) except that neomycin sulfate (2.4 μg/mL) was included in the buffer (300 mM mannitol, 20 mM 2-mercaptoethanol, 5 mM EGTA, 1 mM EDTA, 0.1 mM PMSF, 150 μg mL^{-1} pepstatin A, 100 μg mL^{-1} leupeptin, 1 μg mL^{-1} soybean trypsin inhibitor, 10 mM HEPES−HCl at pH 8).

Toxin Overlay Assays. Protein blot analysis of BBMV preparations was done as described previously (*28*). The BBMV protein (10 μg) was separated by 9% SDS−PAGE and electrotransferred to nitrocellulose membranes. After blocking, the blots were incubated for 2 h with 10 nM Cry1Ac or mutant W545A toxins with or without 25−250

mM GalNAc or *N*-acetylglucosamine (GlcNAc) in washing buffer (1% Tween 20 in PBS) at room temperature. The unbound toxin was removed by washing three times for 10 min in the washing buffer (1 mL), and the bound toxin was identified with polyclonal anti-Cry1Ac (1/10 000; 1 h) and visualized with a goat anti-rabbit antibody coupled with horseradish peroxidase (Sigma, St. Louis, MO) (1/1000; 1 h), followed by SuperSignal chemiluminescence substrate (Pierce, Rockford, IL) as described by the manufacturers.

Determination of Cry1Ac and Mutant W545A Affinities to APN-Enriched Extracts. Apparent dissociation constants (K_D) were determined by competitive ELISA as described (*6*, *29*). BBMV were solubilized as described for *Lymantria dispar* APN purification (*20*). Then, 10 nM Cry1Ac or mutant W545A were incubated with increasing concentrations of APN-enriched extract (from 1 nM to 1 μM) in 100 μL of PBS for 1 h at 25 °C. The incubation mixtures were transferred to 96-well ELISA plates previously coated with 2.5 μg of APN-enriched extract to determine the amount of unbound Cry1Ac or W545A. The ELISA plates were washed three times and detected with anti-Cry1Ac antibody (1:1000) followed by a secondary goat-anti-rabbit-HRP antibody and detected by HRP enzymatic activity. The concentration of APN at which the half-maximal ELISA signal is detected corresponds to the dissociation constant (*6*, *29*). The K_D values were calculated from two replicas of three independent experiments.

Fluorescence Emission and Quenching. The experiments were carried out in an Aminco Bowman Luminescence Spectrometer (Urbana, IL). All measurements were made in a (4 × 10 mm) quartz cuvette at 22 °C. The excitation and emission slits were 4 nm. The excitation wavelength was set at 290 nm, and the emission spectrum was recorded from 300 to 400 nm. The spectra presented are the average of three to four scans and are also corrected for background and dilution.

Fluorescent quenching experiments were performed with I^- (KI). Small-volume aliquots of 4 M KI stock solution, prepared in the protein buffer, were added to the samples and gently stirred. The emission spectra were recorded to check the effect on fluorescence intensity and λ_{max}. As control in KI quenching assays, KCl was added so that the total salt (KI + KCl) concentration remained constant and equal to the highest concentration of KI used. Sodium thiosulfate (800 μM) was added to KI solutions to avoid the formation of I_3^-, which absorbs at the same wavelength as W.

Effective Stern−Volmer constants (K_{SV}) were obtained from the fluorescent data according to the Stern−Volmer equation for dynamic quenching (*30*)

$$F_o/F = 1 + K_{SV}\,(Q), \qquad (1)$$

where F_o and F are the florescence intensities in absence and presence of the quencher, respectively. The value for K_{SV} can be considered to be a reliable reflection of the bimolecular collisional constant for collisional quenching of the W because $K_{SV} = k_q \cdot \tau_o$, where k_q is the bimolecular collisional constant, and τ_o is the lifetime constant in the absence of quencher. However, if all Ws are not equally accessible to the quencher, a modification of Stern−Volmer plot described by the Lehrer equation (*30*) can be used

$$F_o/(F_o - F) = 1/K_{SV}\cdot(Q) + 1/f_a \qquad (2)$$

where $(F_o - F)$ refers to the change in fluorescence intensity upon the addition of the quencher, and f_a refers to the fraction of W accessible to the quencher.

Preparation of Small Unilamellar Vesicles (SUV). Egg-derived-phosphatidyl choline lipids from chloroform stocks (Avanti Polar Lipids, Alabaster, AL) were dried by argon flow evaporation in glass vials at 2.6 μmol total followed by overnight storage under vacuum to remove residual chloroform. The lipids were hydrated in a 2.6 mL of Hepes 10 mM and 150 mM KCl at pH 7.2 buffer by vortexing. To prepare SUV, the lipid suspension was subjected to sonication five times for 5 min in a Branson-1200 bath sonicator (Danbury, CT). SUV were used within 4−5 days upon their preparation.

Insertion of the Pre-Pore Oligomeric Structure into SUV. To analyze the interaction of Cry1Ac with the membrane, the purified oligomeric pre-pore structure was incubated with phosphatidyl choline SUV at different lipid/protein ratios (from 100 to 20000). The mixture was incubated for 30 min at 25 °C in the presence or absence of 75 mM GalNAc or GlcNAc, and the membrane fraction was separated by ultracentrifugation (1h at 100 000*g*), and the fluorescence spectra were recorded in both the supernatant and pellet fractions. The controls of oligomeric Cry1Ac incubated in the absence of the membrane were performed, showing that this protein structure remained in solution under the used experimental conditions. Also, control spectra from SUV alone and in the presence of both sugars were performed under the same conditions and subtracted from the respective protein spectra. These experiments were performed three times.

RESULTS

Mutagenesis of Residue W545, Effect on Toxicity and Binding to BBMV. As mentioned previously, Cry1Ac toxin contains ten W residues, and seven of them are located in domain I, two in domain II, and one in domain III. All Cry1Ac W residues, with the exception of domain III W545, are conserved in the closely related Cry1Ab toxin, which has been previously characterized regarding its W fluorescence in the monomeric and oligomeric structures (*26*). W545 is located close to the GalNAc binding pocket (*21*, *22*). To analyze possible structural changes induced by the binding of GalNAc to Cry1Ac toxin, the W545 residue was substituted by alanine. Wild-type Cry1Ac and the W545A mutated proteins were purified and tested for biological activity against first instar *M. sexta* larvae. Table 1 shows that the mutant W545A retained high toxicity against these insect larvae.

We analyzed the binding of the wild-type and the W545A mutant to BBMV from *M. sexta* by toxin overlay assays. Figure 1A shows that the W545A mutant retained its capacity to interact with the 120 kDa APN and with the 60 kDa alkaline phosphatase proteins, although with less efficiency than that of the wild type Cry1Ac toxin. However, the W545A mutant was still able to interact with the sugar moiety because the binding of this protein competed with BBMV by 250 mM GalNAc in contrast to GlcNAc (250 mM), which did not compete for binding. The competition

Table 1: Toxicity of Cry1Ac and W545A Proteins against First Instar Larvae of *Manduca sexta*

toxin	LC_{50} (ng/cm^2)
Cry1Ac	2.3 (1.4−3.4)[a]
W545A	4.0 (2.9−5.2)

[a] 95% fiducial limits.

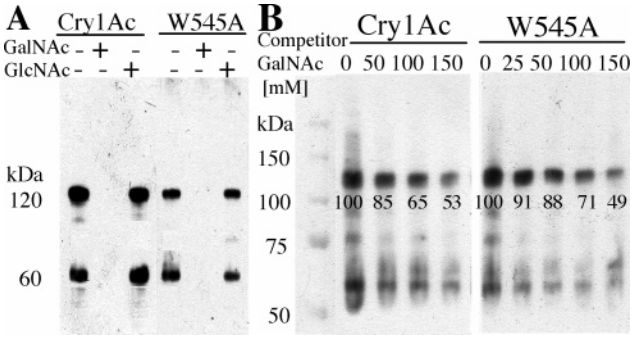

FIGURE 1: Carbohydrate GalNAc competes for the binding of Cry1Ac and mutant W545A to the 120 kDa APN and the 65 kDa alkaline phosphatase receptors. Toxin overlay assays of wild-type and mutant toxins to *Manduca sexta* BBMV. Panel A, competition with 250 mM GalNAc or GlcNAc. Panel B, competition with different mM concentrations of GalNAc. Numbers within images of panel B represent the percentage of the signal relative to Cry1Ac or W545A binding without the competitor as determined by the scanning optical density of the bands in the blots.

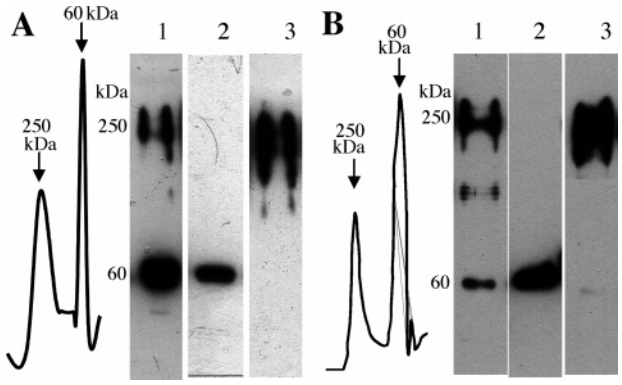

FIGURE 2: Purification of the oligomeric and monomeric forms of Cry1Ac and mutant W545A toxin by size exclusion chromatography. Elution profiles on a Superdex 200 HR 10/30 column. The arrows indicate the elution of 250 and 60 kDa proteins. Western blot of purified monomeric and oligomeric structures: lane 1, Cry1Ac or W545A protoxins proteolitically activated in the presence of scFv73 antibody; lane 2, purified monomeric structures after size exclusion chromatography; lane 3, purified oligomeric structures after size exclusion chromatography. Panel A, Cry1Ac toxin; panel B, mutant W545A.

assays with different concentrations of GalNAc revealed that 150 mM GalNAc displaced 50% binding of the mutant and wild-type proteins to APN and alkaline phosphatase. These results show that Cry1Ac W545A mutation did not affect the interaction with the GalNAc carbohydrate moiety.

To quantitatively analyze the effect of W545A mutation in the binding to *M.sexta* APN, the apparent dissociation constant of the monomer or the oligomer structures to APN was determined. Cry1Ac and W545A protoxins were proteolytically activated in the presence of scFv73 antibody, which mimics a Bt-R_1 Cry1A binding epitope to induce oligomerization (*5*). Figure 2 shows the purified oligomeric and the monomeric forms of Cry1Ac wild-type and mutant

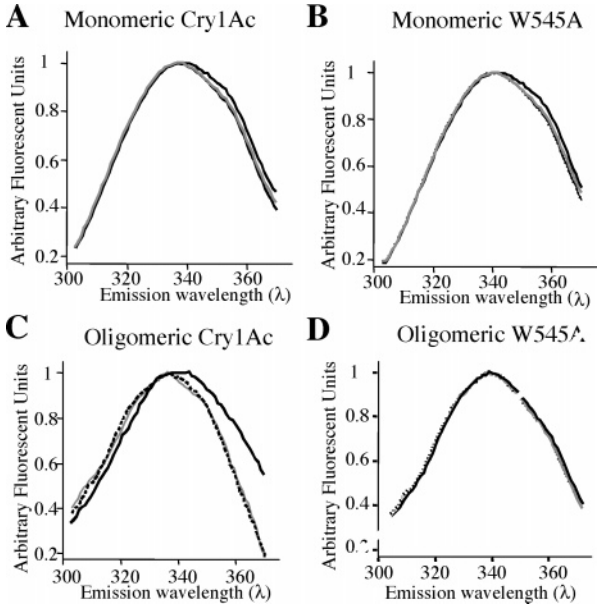

FIGURE 3: Tryptophan fluorescent emission spectra of monomeric or oligomeric structures of Cry1Ac and W545A mutant toxin incubated for 1 h with 150 mM GalNAc or 150 mM GlcNAc carbohydrates. Panel A, monomeric Cry1Ac structure; panel B, monomeric W545A mutant structure; panel C, oligomeric Cry1Ac structure; panel D, oligomeric W545A mutant structure. Thin gray lines, monomeric or oligomeric structures; solid black lines, monomeric or oligomeric structures incubated with GalNAc carbohydrate; broken black line, monomeric or oligomeric structures incubated with GlcNAc carbohydrate.

toxins after size exclusion chromatography. Apparent dissociation constants (K_D) were determined by competitive ELISA as described (*6*, *29*). The W545A monomer showed a slightly lower affinity than the Cry1Ac wild-type monomeric toxin, with an apparent K_D of 150 ± 0.049 nM in contrast to a K_D of 100 ± 0.085 nM determined for the wild-type Cry1Ac-monomeric toxin. Regarding the Cry1Ac-oligomer interaction with APN, we found that the W545A−oligomer bound APN with an apparent dissociation constant (K_D= 10 ± 0.018 nM) higher than that of wild-type Cry1Ac-oligomer (K_D= 1± 0.017 nM).

Steady-State Fluorescence Quenching of W Emission of Cry1Ac and the W545 Mutant Toxin in Aqueous Solution. The W fluorescence of the soluble monomeric and oligomeric forms of Cry1Ac and W545A proteins was analyzed in the presence or absence of GalNAc. Figure 3 shows that the emission spectra of the monomeric structures of Cry1Ac and the W545A mutant were very similar with a maximal of 338 nm, and the incubation with sugar GalNAc induced a small change in the maximal emission to 339 nm. In contrast, the incubation with GlcNAc did not affect the W fluorescence of these proteins. However, the emission spectra obtained with the oligomeric structures of these proteins showed important differences between the wild-type and the mutant proteins. Upon interaction with GalNAc, the wild-type toxin presented a shift of 7 nm in the maximal emission that was not observed with GlcNAc (Figure 3C). The emission spectrum of the oligomeric structure of the W545A mutant was not affected by GalNAc or by GlcNAc moieties, showing a λ maximal of 335 nm (Figure 3D). These results indicated that the emission shift observed in the oligomeric structure upon GalNAc binding was mainly due to structural changes in domain III in the vicinity of W545.

Table 2: Comparison of the Cry1Ac and W545A Mutant Toxin Stern−Volmer Constants (K_{SV}) and the Percentage of W Residues Exposed to the Solvent in Their Corresponding Monomeric or Oligomeric Structures

Cry toxin	toxin structure	GalNAc (150 mM)	K_{SV} (M^{-1})	W exposed to the solvent (%)	Reduction in fluorescence intensity at 500 mM KI (%)
Cry1Ab	monomer	−	1.15 ± 0.19	49.5 ± 9.4	36 ± 1
Cry1Ab	oligomer	−	0.83 ± 0.15	22.9 ± 1.7	31 ± 2
Cry1Ac	monomer	−	0.87 ± 0.06	39.1 ± 8.1	31.7 ± 1.6
Cry1Ac	monomer	+	0.84 ± 0.09	36 ± 6.4	30.3 ± 2.2
Cry1Ac	oligomer	−	0.25 ± 0.02	13.3 ± 1.2	12.3 ± 1.5
Cry1Ac	oligomer	+	0.38 ± 0.03	20.4 ± 2.2	16.4 ± 1.3
Cry1Ac	oligomer in SUV	−	0.18 ± 0.09	10 ± 1.6	9 ± 4.3
Cry1Ac	oligomer in SUV	+	0.35 ± 0.01	17.7 ± 2.4	15.6 ± 0.4
W545A	monomer	−	0.84 ± 0.18	37.2 ± 4.2	31.2 ± 5.1
W545A	monomer	+	0.64 ± 0.06	32 ± 3.6	25.4 ± 1.5
W545A	oligomer	−	0.34 ± 0.04	16.8 ± 0.4	16.4 ± 0.2
W545A	oligomer	+	0.32 ± 0.03	15.5 ± 2.8	15.0 ± 2.3
W545A	oligomer in SUV	−	0.158 ± 0.03	4.5 ± 0.56	7.4 ± 0.45
W545A	oligomer in SUV	+	0.123 ± 0.01	4.7 ± 0.3	7.2 ± 0.2

To analyze the exposure of the W residues of the monomeric and the oligomeric structures upon GalNAc binding, the quenching of W residues by iodide (I^-) was determined. The iodide quencher yielded linear Stern−Volmer plots, and the apparent dynamic quenching constants K_{SV} derived from the slope of these plots are presented in Table 2. The effective K_{SV} for I^- quenching of the Cry1Ac monomeric toxin was 0.87 ± 0.06 M^{-1}. The Lehrer analysis gave an accessibility factor (f_a^{-1}) of 2.5 ± 0.43, indicating that ∼39.1 ± 8% of the W residues are accessible to the solvent (Table 2). The monomeric structure of the mutant W545A showed a similar amount of W exposed to the solvent (37.2 ± 4%), with an accessibility factor of 2.6 ± 0.30, indicating an exposure of W residues similar to that of Cry1Ac protein and confirming that W545 is not exposed to the solvent in the monomeric Cry1Ac toxin structure.

The quenching analysis performed with the oligomeric structures of Cry1Ac and mutant W545A showed that the W residues are less exposed to the solvent in these protein structures than that in their corresponding monomeric structures. The accessibility factor f_a^{-1} of 7.51 ± 0.6 for the Cry1Ac and 5.95 ± 0.1 for the mutant W545A indicated that only 13.3 ± 1% of the W residues of the Cry1Ac oligomer and 16.8 ± 0.4 of the mutant W545A are accessible to I^-.

When the oligomeric structures of these proteins were incubated with GalNAc, there was a significant change in the amount of W exposed to the solvent of the wild-type protein. The accessibility factor f_a^{-1} was reduced to 4.9 ± 0.4, indicating a 7% increase in the amount of W exposition to the solvent, in contrast to the mutant toxin that did not change, indicating again that the structural changes observed in the wild-type oligomeric structure are mainly due to changes in the vicinity of W545 (Table 2).

Analysis of the W Fluorescence of Cry1Ac and W545A Membrane-Inserted Oligomers. To determine the effect of GalNAc binding in the Cry1Ac membrane-inserted oligomer, pure oligomeric structures of Cry1Ac and W545A were incubated with phosphatidyl choline SUV. This membrane model was chosen because the interference of fluorescence emission is minimal between W and these vesicles and also because previous studies demonstrated that oligomeric Cry1Ab toxin inserts efficiently in this membrane lipid, forming stable ionic pores (*26*).

The accessibility of W residues when the oligomeric Cry1Ac was inserted into SUV was explored by steady-state fluorescence quenching using I^-. After the incubation period, the membrane fraction was separated by ultracentrifugation, and emission fluorescence was recorded in both the supernatant and pellet fractions. Table 2 shows a reduced K_{SV} constant value for both membrane-associated oligomeric proteins, compared with the K_{SV} value obtained in aqueous solution. The accessibility factor f_a^{-1} of 10.0 ± 1.3 and 22.2 ± 1.1 for the Cry1Ac and mutant W545A, respectively, indicated a different W exposure for these two protein molecules. The estimation of the percentage of W exposed to the solvent for Cry1Ac was 10.0 ± 1.6%, whereas for mutant W545A, it was 4.5 ± 0.5%. This result suggests that in contrast to most W residues located in domain I and II, the W545 remains accessible to the solvent in the membrane bound state.

The interaction of the membrane bound proteins with GalNAc induced significant changes in the amount of W exposed to the solvent of the wild-type protein. The accessibility factor f_a^{-1} of 5.6 ± 0.6 indicated that 17.7 ± 2.4% of the W residues are exposed to the solvent, in contrast to the mutant toxin that did not change upon interaction with GalNAc. These data suggest that Cry1Ac had a conformational change of domain III, triggered by interaction with ligand sugar GalNAc. This effect was not observed with GlcNAc.

Membrane Insertion of the Oligomeric Cry1Ac Structure. To analyze the effect of GalNAc interaction on the efficiency of toxin insertion into the membrane, the binding of the oligomer structure of Cry1Ac to membrane was determined using phosphatydilcholine SUV. Different lipid/protein ratios (from 100 to 20 000) were assayed with pure Cry1Ac oligomeric structure in the presence or absence of GalNAc. After the incubation of the oligomeric Cry1Ac toxin with SUV, the membrane fraction was separated by ultracentrifugation, and W spectra were recorded in the supernatant and in the pellet fractions. Figure 4 shows that the threshold limit for the partitioning of the oligomer in the presence of GalNAc was a lipid/protein ratio of 800 in contrast to a threshold limit of 2000 when GalNAc was not present in the assay. This result shows that Cry1Ac pre-pore oligomer inserts more efficiently into phosphatydilcholine SUV in the presence of GalNAc.

DISCUSSION.

It has been proposed that the Cry1A toxins interact sequentially with at least two different receptors during their interaction with the target membrane. In this model, Cry1A monomeric toxins interact first with a Bt-R_1 receptor leading to the formation of pre-pore oligomers (*5*), which then bind to GPI-anchored receptors (APN or alkaline phosphatase) resulting in the insertion of the pre-pore oligomers into membrane microdomains (*6*, *13*). In the case of Cry1Ac toxin, the interaction with the GPI-anchored receptors is through the GalNAc moiety (*17*−*19*). Previously, we showed

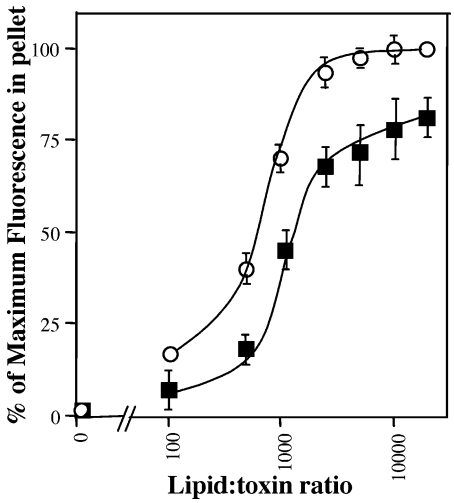

FIGURE 4: Insertion of the oligomeric structure of Cry1Ac into phosphatidyl choline SUV membranes. The percentage of maximum fluorescence recorded in the membrane pellet obtained after centrifugation for 1 h at 100 000*g* of the Cry1Ac oligomeric structure incubated with the SUV in the presence (○) or absence (■) of 150 mM GalNAc as a function of lipid concentration. The protein concentration was kept constant (5 nM), and the lipid/protein ratio is a molar ratio. The controls of oligomeric Cry1Ac centrifuged without the SUVs were included in this Figure.

that the pre-pore oligomer of Cry1Ab toxin has a higher binding affinity to APN compared to that of the monomeric toxin. In this work, we quantified the binding affinity of Cry1Ac oligomer to APN, showing a similar 100-fold increase compared to that of the monomeric toxin. We have hypothesized that the interaction of the pre-pore oligomer with the APN receptor could trigger a more efficient membrane insertion of the pre-pore because the cleavage of APN by phosphatidylinositol specific phospholipase C decreased the levels of the Cry1Ab oligomer in membrane microdomains (*6*) and drastically reduced the pore-formation activity of the toxin (*14*). In addition, APN incorporation into the lipid bilayer enhanced Cry1Aa pore-formation activity (*15*). The objective of this work was to analyze the conformational changes of Cry1Ac during the interaction with APN receptor. The GalNAc sugar was used instead of the whole receptor because GalNAc is a binding determinant of Cry1Ac to APN (*17*, *18*). To compare Cry1Ac to other members of Cry1A toxin family, as the Cry1Ab toxin, we mutated W545 to alanine because only Cry1Ac has this W. This mutation is also important for analyzing possible structural changes induced by the binding of GalNAc to the Cry1Ac toxin because W545 is located close to the GalNAc binding pocket (*20*, *21*).

The W545A mutant resulted in a protein that preserved significant biological activity against *Manduca sexta* larvae and, therefore, was suitable for this study. The same Cry1Ac mutation was previously characterized, showing a 50-fold reduction in the insecticidal activity against *Lymantria dispar* larvae (*20*). In addition, the Cry1Ac W545A mutant did not bind to immobilized *L. dispar* APN (*20*). In this work, we show that Cry1Ac W545A mutant is toxic to *M. sexta* larvae and is capable of interacting with *M. sexta* APN. These data could indicate that APN from *L. dispar* may have important differences with *M. sexta* APN and that the interaction of Cry1Ac with *L. dispar* APN determines the insecticidal effect against this insect. We report here that the W545A interaction with *M. sexta* APN depends on GalNAc because this sugar competed with the binding of W545A to APN, similar to the wild-type Cry1Ac toxin (Figure 1).

The analysis of the W fluorescence of the Cry1Ac toxin indicated that the W residues of Cry1Ac have a different exposure to the solvent when compared with that of the Cry1Ab toxin. The W quenching analysis of Cry1Ab performed with KI showed that Cry1Ab monomeric toxin has 49.5 ± 9% of W residues exposed to the solvent (*26*); these residues correspond to some W residues located in domain I because the two W residues of domain II are completely buried in the interior of the protein (*8*, *9*). Despite the fact that Cry1Ac contains an additional W residue (W545) compared to Cry1Ab, the monomeric structure of Cry1Ac has a lower amount of W residues exposed to the solvent (39 ± 8%). These data indicate that the monomeric Cry1Ac displays a more compact structure than the Cry1Ab toxin. The oligomeric structure of Cry1Ac also has a reduced amount of W exposed to the solvent (13.3 ± 1.2%) compared with the Cry1Ab oligomeric structure (22.9±1.7%) (*26*). However, if we compare the amount of W residues that were buried upon oligomerization of these proteins, we found a similar value of 27% reduction of W residues exposed to the solvent for Cry1Ab and 26% for Cry1Ac, suggesting the similar conformational change of both toxins.

The Cry1Ac toxin binding to GalNAc specifically has a marked effect on the exposure of W545 in the pre-pore oligomer, in contrast with the monomer. First, the maximal emission wavelength of the oligomeric Cry1Ac increased 7 nm after GalNAc binding, suggesting a higher exposure of some W residues to the solvent (Figure 3C). Second, the quenching analysis performed with KI confirmed that 7% of the W residues that were buried in the oligomeric structure became accessible to the quencher upon contact with the ligand GalNAc (Table 2). These effects were not observed with GlcNAc, indicating that the conformational changes were triggered by the specific interaction with the ligand GalNAc. The conformational change was due to changes on the polarity on the vicinity of W545 in domain III of the oligomeric structure of Cry1Ac because GalNAc binding had no effect on the fluorescence of the oligomeric structure of the mutant W545A toxin (Figure 3 and Table 2) despite the fact that the mutant W545A was able to bind the GalNAc sugar (Figure 1). These data could indicate that there was no major structural change in the vicinity of the W residues located in domains I and II upon GalNAc binding. Nevertheless, because we have analyzed the fluorescence of nine W residues at the same time, it could be possible that structural changes on these domains do no reflect net changes in the polarity of W residues. To better analyze the effect of GalNAc binding on the structure of domain I and II, it will be necessary to construct Cry1Ac mutants that retain only one W residue (or few W residues) and that remain active (work in progress).

Analysis of W fluorescence of the membrane-inserted Cry1Ac oligomer indicated that a small proportion of W residues in wild-type and mutant proteins remain exposed to the solvent (10.0 ± 1.6% for Cry1Ac and 4.5 ± 0.5% for the mutant W545A) in contrast to the Cry1Ab oligomer, where no W residues were exposed to the solvent when the oligomeric-Cry1Ab was inserted into the membrane (*26*). These data suggest that the insertion into the membrane of

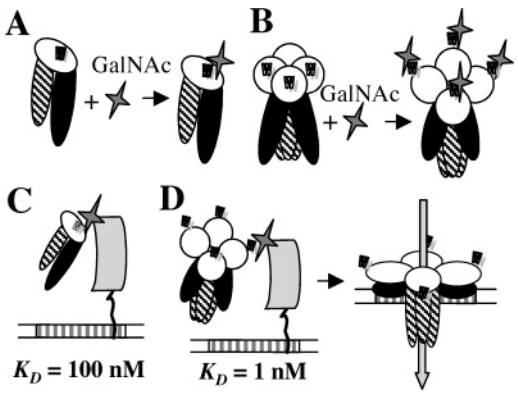

FIGURE 5: Model of the pore formation of Cry1Ac toxin. Domain I is represented by striped ovals, domain II by black ovals, and domain III by white ovals. The tryptophan 545 residue is represented by w (lower case). APN is represented by a gray figure, and the lipid bilayer containing the membrane microdomains is shown in the Figure. Panel A, binding of GalNAc to the monomeric Cry1Ac toxin; this interaction did not affect the W fluorescence of the toxin. Panel B, binding of GalNAc to the oligomeric Cry1Ac; this interaction resulted in a conformational change where W545 is exposed to the solvent. Panel C, binding of monomeric Cry1Ac to APN and its corresponding K_D; panel D, high affinity binding of the oligomeric Cry1Ac to APN, which facilitates membrane insertion and pore formation.

Cry1Ac is slightly different from that of Cry1Ab. Quenching analysis of W florescence of the membrane-inserted Cry1Ac oligomer also showed an increase in the amount of W residues exposed to the solvent upon GalNAc binding (Table 2). This change in W exposure was not observed on the W545A membrane-inserted oligomer, suggesting that the exposed W residue in wild-type Cry1Ac oligomer corresponds to W545. On the basis of these data, we propose that domain III, or part of it, is located in the surface of the membrane. This conclusion is in agreement with FRET analysis of W residues to ANS in partially denatured membrane-bound Cry1Ab oligomer that indicated that domains II and III remained on the surface of the membrane in contrast to domain I, which was protected by the lipids, provably inserted into the membrane (*31*).

We have shown that the Cry1Ab (*6*) and Cry1Ac oligomers (this work) have a high binding affinity to the APN receptor, and we speculated that this interaction might be important for the efficient insertion of the toxin into the membrane (*6*). Our work shows that GalNAc binding specifically affects the exposure of W545 to the solvent in the pre-pore oligomer in contrast to the monomer where GalNAc binding did not affect the fluorescence of this residue. Overall, the conclusions are that a subtle conformational change in the GalNAc binding pocket in the pre-pore oligomer could explain the increased binding affinity of the Cry1Ac pre-pore to APN. Finally, we analyzed the effect of GalNAc binding on the efficiency of membrane insertion of the Cry1Ac pre-pore. Our data indicate that GalNAc binding to the pre-pore oligomer facilitated its insertion into the membrane (Figure 4), suggesting that receptor binding could trigger conformational changes in the protein that are important for membrane insertion. On the basis of this data, we propose a revised model for the pore formation of the Cry1Ac toxin (Figure 5). In Figure 5, we show that the binding of GalNAc to the monomeric Cry1Ac toxin does not affect the W fluorescence of the molecule (Figure 5, panel A). In contrast, the binding of GalNAc to the oligomeric structure of Cry1Ac has a marked effect on the exposure of W545 (Figure 5, panel B). The conformational change in domain III due to GalNAc interaction could be responsible of the higher affinity of the oligomeric Cry1Ac to APN (Figure 5, panels C and D). Finally, the interaction of Cry1Ac pre-pore oligomer with APN receptor facilitates membrane insertion and pore formation (Figure 5, panel D). The APN−oligomer interaction may be especially critical when low toxin protein concentrations reach the midgut epithelium, conditions *in vivo* that may be present where the Cry toxins are exposed to high concentrations of proteases in the larval midgut lumen.

ACKNOWLEDGMENT

Our thanks to Lizbeth Cabrera and Oswaldo López for technical assistance.

REFERENCES

1. Schnepf, E., Crickmore, N., Van Rie, J., Lereclus, D., Baum, J. R., Feitelson, J., Zeigler, D., and Dean, D. H. (1998) *Bacillus thuringiensis* and its pesticidal crystal proteins, *Microbiol. Mol. Biol. Rev. 62*, 705−806.
2. de Maagd, R. A., Bravo, A., and Crickmore, N. (2001) How *Bacillus thuringiensis* has evolved specific toxins to colonize the insect world, *Trends Genet. 17*, 193−199.
3. Bravo, A., Jansens, S., and Peferoen, M. (1992) Immunocytochemical localization of *Bacillus* thuringiensis insecticidal crystal proteins in intoxicated insects, *J. Invertebr. Pathol. 60*, 237−247.
4. Choma, C. T., Surewicz, W. K., Carey P. R., Pozsgay, M., Raynor, T., and Kaplan, H. (1990) Unusual proteolysis of the protoxin and toxin from *Bacillus thuringiensis.* Structural implications, *Eur. J. Biochem. 189*, 523−527.
5. Gómez, I., Sánchez, J., Miranda, R., Bravo, A., and Soberón, M. (2002) Cadherin-like receptor binding facilitates proteolytic cleavage of helix α-1 in domain I and oligomer pre-pore formation of *Bacillus thuringiensis* Cry1Ab toxin, *FEBS Lett. 513*, 242−246.
6. Bravo, A., Gómez, I., Conde, J., Muñoz-Garay, C., Sánchez, J., Miranda, R., Zhuang, M., Gill, S. S., Soberón, M. (2004) Oligomerization triggers binding of a *Bacillus thuringienis* Cry1Ab pore-forming toxin to aminopeptidase *N* receptor leading to insertion into membrane microdomains, *Biochim. Biophys. Acta* 1667, 38−46.
7. Boonserm, P., Davis, P., Ellar, D. J., Li, J. (2005) Crystal structure of the mosquito-larvicidal toxin Cry4Ba and its biological implications, *J. Mol. Biol. 348*, 363−382.
8. Grochulski, P., Masson, L., Borisova, S., Pusztai-Carey, M., Schwartz, J. L., Brousseau, R., and Cygler, M. (1995) *Bacillus thuringiensis* CryIA(a) insecticidal toxin-crystal structure and channel formation, *J. Mol. Biol. 254*, 447−464.
9. Li, J., Carroll, J., and Ellar, D. J. (1991) Crystal structure of insectidicidal delta-endotoxin from *Bacillus* thuringiensis at 2.5 Å resolution, *Nature* 353, 815−821.
10. Morse, R. J., Yamamoto, T., and Stroud, R. M. (2001) Structure of Cry2Aa suggests an unexpected receptor binding epitope, *Structure 9*, 409−417.
11. Vadlamudi, R. K., Weber, E., Ji, I., Ji, T. H., and Bulla, L. A., Jr. (1995) Cloning and expression of a receptor for an insecticidal toxin of *Bacillus thuringiensis*, *J. Biol. Chem. 270*, 5490−5494.
12. Knight, P., Crickmore, N., and Ellar, D. J. (1994) The receptor for *Bacillus thuringiensis* CryIA(c) delta-endotoxin in the brush border membrane of the lepidopteran *Manduca sexta* is aminopeptidase *N*, *Mol. Microbiol. 11*, 429−436.
13. Zhuang, M., Oltean, D. I., Gomez, I., Pullikuth, A. K., Soberon, M., Bravo, A., Gill, S. S. (2002) *Heliothis virescens* and *Manduca sexta* lipid rafts are involved in Cry1A toxin binding to the midgut epithelium and subsequent pore formation, *J. Biol. Chem. 277*, 13863−13872
14. Lorence, A., Darszon, A., and Bravo, A. (1997) The pore formation activity of *Bacillus thuringiensis* Cry1Ac toxin on *Trichoplusia ni* membranes depends on the presence of aminopeptidase *N*, *FEBS Lett. 414*, 303−307.

15. Schwartz, J. L., Lu, Y. J., Sohnlein, P., Brousseau, R., Laprade, R., Masson, L., Adang, M. J. (1997) Ion channels formed in planar lipid bilayers by *Bacillus thuringiensis* toxins in the prescence of *Manduca sexta* midgut receptors, *FEBS Lett. 412*, 270−276.
16. de Maagd, R. A., Bravo, A., Berry, C., Crickmore, N., and Schnepf, H. E. (2003) Structure, diversity and evolution of protein toxins from spore-forming entomopathogenic bacteria, *Annu. Rev. Genet. 37*, 409−433
17. Masson, L., Lu, Y.-J., Mazza, A., Brosseau, R., and Adang, M. J. (1995*)* Kinetics of *Bacillus* thuringiensis toxin binding with brush border membrane vesicles from susceptible and resistant larvae of *Plutella xylostella*, *J. Biol. Chem. 270*, 20309−20315.
18. Cooper, M. A., Carroll, J., Travis, E., Williams, D. H., and Ellar, D. J. (1998) *Bacillus thuringiensis* Cry1Ac toxin interaction with *Manduca sexta* aminopeptidase N in a model membrane environment, *Biochem. J. 333*, 677−683.
19. Jurat-Fuentes, J. L., and Adang, M. J. (2004) Characterization of a Cry1Ac-receptor alkaline phosphatase in susceptible and resistant *Heliothis virescens* larvae, *Eur. J. Biochem. 271*, 3127−3135.
20. Jenkins, J. L., Lee, M. K., Valaitis, A. P., Curtiss, A., and Dean, D. H. (2000) Bivalent sequential binding model of a *Bacillus thuringiensis* toxin to gypsy moth aminopeptidase *N* receptor, *J. Biol. Chem. 275*, 14423−14431.
21. Burton, S. L., Ellar, D. J., Li, J., and Derbyshire, D. J. (1999) *N*-acetylgalactosamine on the putative insect receptor aminopeptidase N is recognised by a site on the domain III lectin-like fold of a *Bacillus* thuringiensis insecticidal toxin, *J. Mol. Biol. 287*, 1011−22.
22. Lee, M. K., You, T. H., Gould, F. L., and Dean, D. H. (1999) Identification of residues in domain III of *Bacillus thuringiensis* Cry1Ac toxin that affect binding and toxicity, *Appl. Environ. Microbiol. 65*, 4513−4520.
23. Li, J., Derbyshire, D. J., Promdonkoy, B., and Ellar, D. J. (2001) Structural implications for the transformation of the *Bacillus thuringiensis* δ-endotoxins from water-soluble to membrane-inserted forms, *Biochem. Soc. Trans. 29*, 571−577.
24. Aronson, A. I., Wu, D., and Zhang, C. H. (1995) Mutagenesis of specificity and toxicity regions of *Bacillus thuringiensis* protoxin gene, *J. Bacteriol. 177*, 4059−4065
25. Thomas, W. E., and Ellar, D. J. (1983) *Bacillus thuringiensis* var. *israelensis* crystal delta-endotoxin: effects on insect and mammalian cells *in vitro* and *in vivo*, *J. Cell. Sci. 60*, 181−197.
26. Rausell, C., Muñoz-Garay, C., Miranda-CassoLuengo, R., Gómez, I., Rudiño-Piñera, E., Soberón, M., and Bravo, A. (2004) Tryptophan spectroscopy studies and black lipid bilayer analysis indicate that the oligomeric structure of Cry1Ab toxin from *Bacillus thuringiensis* is the membrane-insertion intermediate, *Biochemistry. 43*, 166−174.
27. Wolfersberger, M., Lüthy, P., Maurer, A., Parenti, P., Sacchi, F. V., Giordana, B., and Hanozet, G. M. (1987) Preparation and partial characterization of amino acid transporting brush border membrane vesicles from the larval midgut of the cabbage butterfly (*Pieris brassicae*), *Comp. Biochem. Physiol., A 86*, 301−308.
28. Aranda, E., Sanchez, J., Perferoen, M., Güereca, L., and Bravo, A. (1996) Interaction of *Bacillus* thuringiensis crystal protein with the migdut epithelial cells of *Spodoptera frugiperda* (Lepidoptera: Noctuidae), *J. Invertebr. Pathol. 68*, 203−212.
29. Hardy, F., Djavadi-Ohaniance, L., and Goldberg, M. E. (1997) Measurement of antibody/antigen association rate constants in solution by a method based on the enzyme-linked immunosorbent assay, *J. Immunol. Methods. 200*, 155−159.
30. Lakowicz, J. (1983) Quenching of fluorescence, in *Principles of Fluorescence Spectroscopy* (Lakowicz, J., Ed.) pp 258−297, Plenum Press, New York.
31. Rausell, C., Pardo-López, L., Sánchez, J., Muñoz-Garay, C., Morera, C., Soberón, M., and Bravo, A. (2004*)* Unfolding events in the water-soluble monomeric Cry1Ab toxin during transition to oligomeric pre-pore and membrane inserted pore channel, *J. Biol. Chem 279*, 55168−55175.

BI060297Z